JOURNAL OF AGRICULTURAL AND FOOD CHEMISTRY

ARTICLE

pubs.acs.org/JAFC

Mapping Brain Activity Induced by Olfaction of Virgin Olive Oil Aroma

Diego L. García-González,*,† Jorge Vivancos,‡ and Ramón Aparicio†

†Instituto de la Grasa (CSIC), Padre García Tejero 4, E-41012 Sevilla, Spain

‡Hospital San Juan de Dios, Avda. San Juan de Dios s/n, E-41930, Bormujos, Spain

ABSTRACT: The difficulty of explaining sensory descriptors of virgin olive oil aroma by the analysis of volatile compounds is partially due to the subjective opinions of panelists and the lack of information of the neural mechanisms that ultimately produce a sensory perception. In this study the technique of functional magnetic resonance imaging (fMRI) has been applied to study brain activity during the smelling of virgin olive oil of different qualities. The volatile compounds of the samples were analyzed by solid-phase microextraction gas chromatography to explain the differences in the aromas presented to the subjects during the fMRI experiments. Comparing the pleasant and unpleasant aromas, the most evident differences in brain activity were found at the anterior cingulate gyrus (Brodmann area 32) and at the temporal lobe (Brodmann area 38). The activations were also observed when subjects smelled dilutions of heptanal and hexanoic acid, both compounds being responsible for off-flavors. Other areas were inherent to the olfaction task (e.g., Brodmann area 10) and to the intensity of the aroma (Brodmann area 6).

KEYWORDS: virgin olive oil, volatiles, aroma, fMRI, brain imaging

INTRODUCTION

Food aroma is regarded as one of the most important factors determining consumer acceptability, and consequently, it has an enormous economical impact on price. The economical importance of food aroma and its effect on overall quality explain the increasing interest for new objective methods of aroma analysis. Particularly, virgin olive oil aroma is also a sensory property that must be characterized by law according to the official method of sensory assessment.[1] This methodology, extensively described in the International Olive Council (IOC) regulations, was developed and validated to overcome the subjective component of panelist opinions by appropriate data processing. In addition to the perfection in data management and the standardization of the procedure, the sensory assessment by panelists still has the drawback of including certain subjective information. The subjective bias of sensory assessment is even more evident when the scores given by panel tests from different countries are compared. Consequently, intensive research has pursued the development of methods for the analysis of the flavor compounds responsible for the aroma[2,3] to acquire objective and univocal information of sensory quality. However, the most updated methodologies of flavor analysis still fail to reproduce the same information provided by sensory assessment. Several reasons explain the gap between instrumental analysis and sensory assessment. The first reason is the high complexity of volatile compounds in virgin olive oil and many other foods, which constitutes a resolution challenge for the current chromatographic techniques.[4] The second reason is the kinetic component of the flavor release occurring during eating and swallowing and influenced by many factors, such as saliva composition and mouth movements. These factors modulate the final sensory perception, and they are not taken into account in most of methodologies for flavor analysis. Finally, little is known about the physiological mechanisms by which flavor compounds result in neural activation and ultimately give rise to sensory perception. The scrutiny of those mechanisms by postreceptor studies with the main purpose of explaining the sensory quality of foods has been scarcely addressed. The application of medical techniques such as positron emission tomography (PET) and functional magnetic resonance imaging (fMRI) in the service of food science has opened a new research field in flavor chemistry that complements the chemical/sensory studies on food quality.

The acquisition of brain activity images with fMRI is based on the magnetic resonance of protons in living tissues.[5] Neural activity is associated with an increase in blood flow. As a consequence, the concentration of deoxyhemoglobin decreases, which is reflected by an increase in the relaxation time and the magnetic resonance signal measured by fMRI. Data from fMRI experiments are analyzed with a contrast analysis[6] that assumes the hypothesis of greater activity during a cognitive process compared to the rest state.[7] Thus, the stimulus is sequentially presented to a subject alternating with rest periods in a block design (or paradigm) in an ON/OFF frame. In addition to assuming a lower brain activity during rest periods, another important assumption is that the timing at which the neural responses are registered matches the time specified in the paradigm.[8] Furthermore, the stimulus needs to be presented to the individual enough times to get a reliable statistical significance.[9] Prior to studying the statistical differences between the signals acquired at ON/OFF periods, the functional and structural images of the brain are processed to avoid artifacts due to slight movements or other phenomena not related to the cognitive process under study.[6] The image processing constitutes the most time-consuming and tedious step in fMRI analysis, which has led to intensive research oriented toward the development of new software that is more powerful and versatile for all the applications.[10] The software packages Analysis of Functional

Received: May 26, 2011
Accepted: August 12, 2011
Revised: August 11, 2011
Published: August 12, 2011

NeuroImages (AFNI),[11] FSL,[8] and SPM[6] are among the most widespread, and they also allow for intercomparison studies between stimuli and individuals through the normalization of the brain images.

The high spatial resolution of fMRI has significantly contributed to the understanding of all the cognitive processes, including the olfaction tasks.[10,12] However, the study of the neural connectivity induced by olfaction involves more difficulty than the study of other cognitive tasks.[13] The high number of variables in the presentation of the odorants (e.g., time, concentration of odorant, carrier gas flow, and humidity), together with the heterogeneity of the magnetic field in the olfactory cortex because of the cerebral bone structures, partially explain this difficulty. Furthermore, the samples may be presented to induce an orthonasal and/or retronasal stimulation,[12] which introduces an additional source of variability. Therefore, the studies of the neural activities induced by olfaction require the use of an optimized system of odorant delivery to be reproducible throughout all the experiments. Thus, Cerf-Ducastel and Murphy[9] proposed a protocol for functional studies of olfaction and taste, while other authors have proposed a delivery system for combined studies of odor and taste based on sprayed liquids.[14] In general terms, the functional studies of olfaction have described activations in the primary olfactory cortex (mainly piriform cortex) and its projection to the secondary olfactory cortex (insula, entorhinal cortex, orbitofrontal cortex, thalamus, hypothalamus),[14] although some inconsistencies due to artifacts or the habituation effect have been described.[10]

Despite the extensive studies on functional neuroimaging of olfaction, most of the studies are based on the delivery of simple substances that are strongly odorant, such as citral,[15] vanilla,[16] geranyl acetate,[17] lavender oil,[18] etc. Few studies have been focused on the food aroma produced by a complex mixture of volatile compounds producing a mild olfactory perception. Coffee, tomato juice, grapefruit, and chocolate are among the foods that have been examined in neuroimaging studies of olfaction/taste.[19,20] Nevertheless, the information of the neural mechanism as to why a food aroma results in a pleasant or unpleasant perception depending on the sensory quality is incomplete. In this respect, Royet et al.[21] studied the brain activity of 126 odorants, some of which were food aromas. These odorants were classified as pleasant and unpleasant, and some differences were found in the brain activities stemming from these two groups.

Assuming that brain activity is different according to the pleasantness or unpleasantness of the aroma,[17,21] it would be expected to find differences in the neuroimages obtained during the smelling of virgin olive oils qualified with different sensory descriptors and the chemical compounds that are sensory markers of three well-known virgin olive oil sensory defects. The flavor of virgin olive oil is among the most studied from a sensory/chemical perspective,[2,22] which provides a further advantage in the chemical interpretation of fMRI results to associate the olfactory perception and the volatile compounds that are responsible for the aroma.

MATERIALS AND METHODS

Samples and Chemicals. Six samples of virgin olive oil (VOO) were selected for the fMRI studies. No sensory defect was detected in three of them, and in consequence, they were qualified as extra virgin olive oil. These three samples were purchased as "premium quality oils", which means that they have highly pleasant green-fruity attributes. These three oils were of varieties Royal, Arbequina, and Picual, characterized with green-fruity, green-tomato, and green-lawn attributes, respectively. On the contrary, the other three oils were characterized by the sensory defects rancid, fusty, and winey.

All the standards of volatile compounds were purchased from Sigma-Aldrich Chemical Co. (St. Louis, MO).

Determination of Volatile Compounds. Volatile compounds were analyzed by solid-phase microextraction gas chromatography.[24] Olive oil samples (2 g) spiked with 2.6 mg/kg of 4-methyl-2-pentanol (internal standard) were placed in a 20 mL glass vial, tightly capped with a polytetrafluoroethylene (PTFE) septum, and left for 10 min at 40 °C to allow for the equilibration of the volatiles in the headspace. After the equilibration time, the septum covering each vial was pierced with a solid-phase microextraction (SPME) needle, and the fiber was exposed to the headspace for 40 min. When the process was completed, the fiber was inserted into the injector port of the gas chromatograph (GC). The temperature and time of the preconcentration step, carried out on a Combipal (CTC Analytics AG, Zwingen, Switzerland), were automatically controlled by the software Workstation version 5.5.2 (Varian, Walnut Creek, CA). The SPME fiber (1 cm length and 50/30 μm film thickness) was purchased from Supelco (Bellefonte, PA), and it was endowed with the Stable Flex stationary phase of divinylbenzene/carboxen/polydimethylsiloxane (DVB/CAR/PDMS). The fiber was previously conditioned following the instructions of the supplier.

The volatiles absorbed by the fiber were thermally desorbed in the hot injection port of a GC for 5 min at 260 °C with the purge valve off (splitless mode) and deposited onto a TR-WAX capillary column (60 m $\times$ 0.25 mm i.d., 0.25 μm coating; Teknokroma, Barcelona, Spain) of a Varian 3900 gas chromatograph with a flame ionization detector (FID). The carrier gas was hydrogen, at a flow rate of 1.5 mL/min. The oven temperature was held at 40 °C for 10 min and then programmed to rise 3 °C/min to a final temperature of 200 °C, where it was held for 10 min to eliminate the memory effect of the capillary column. The signal was recorded and processed with the WorkStation (version 5.5.2) software. Each sample was analyzed in duplicate.

The identification of the volatile compounds was first carried out by mass spectrometry and later checked with standards.[23] The assessment of the aroma notes and the determination of the recovery factors were carried out as explained in a previous work.[23,24]

Sensory Assessment. The sensory evaluation of VOO samples was carried out in accordance with the official method for the olive oil sensory assessment.[1] A total of 15 mL of each sample was kept in standardized glasses at 29 $\pm$ 2 °C for 15 min and then evaluated by five fully trained assessors. Assessors were free to qualify VOOs with their own sensory descriptors in addition to those described in the official method.[1] These free-choice sensory descriptors were "banana", "artichoke", "cut green lawn", "wild flowers", "apple", "green tomato", and "cream". For negative attributes they were "old peanut butter" and "wax crayons" for rancid oil, "gym clothes" and "decomposing olives" for fusty oil, and "nail polish" for winey-vinegary.

Presentation of Samples for fMRI Experiments. A gas-flow olfactometer was designed for the presentation of the samples to the subjects. This olfactometer (Figure 1) was composed of an air source equipped with a flowmeter (Restek Corp., Bellefonte, PA), a PTFE T-connector (Omnifit Ltd., Cambridge, U.K.), a sample vial of 100 mL, an empty vial of the same volume, a solenoid 24 V three-way valve (Omnifit Ltd., Cambridge, U.K.), and a nasal mask. The air source, the vials, and the valve were connected with PTFE tubes with an internal diameter of 5 mm. The open/close valve periods were automatically controlled by an in-house adjustable valve controller equipped with timer circuits (Cebek S.A., Barcelona, Spain). The valve controller was the only part of the olfactometer that was outside of the magnetic room, and it was connected to the rest of the olfactometer system through a RS-232 connector plugged into the interface electric board. The latter allows

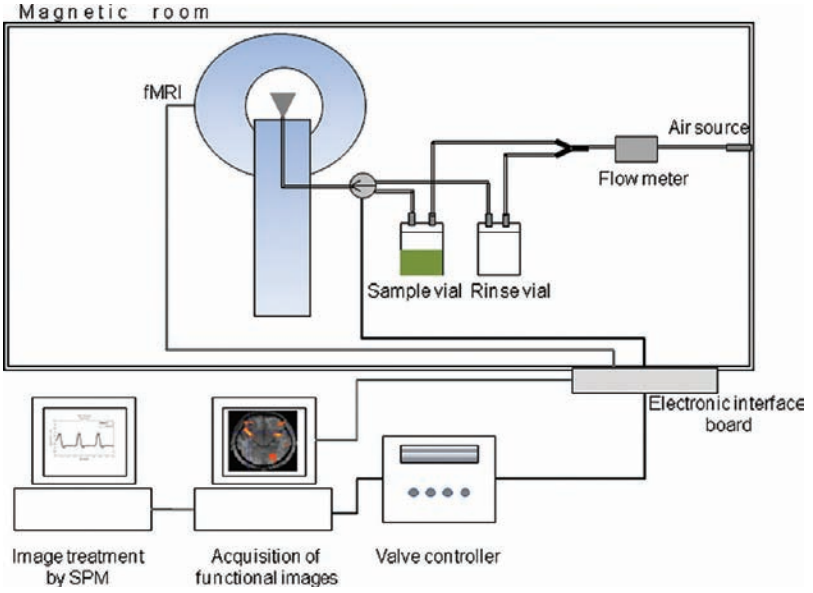

Figure 1. Scheme of the olfactometer designed to deliver the virgin olive oil aroma to the subjects.

connecting cables to the room without any risk of affecting the magnetic field. Therefore, the olfactometer within the magnetic room had a thin wire and a small metallic piece in the solenoid valve as the only metallic parts of the design, the rest being made of PTFE, PVC, and glass. It was proven that these metallic parts did not affect the fMRI measurements.

Fourteen subjects (7 male and 7 female) with an age range from 28 to 47 years old (mean = 34, standard deviation = 17) were selected for the fMRI studies. Each subject participated in the experiences for no longer than 45 min including three functional runs. The stimuli (aromas released from 5 g of virgin olive oil) were presented to the subject for 3 min, alternating with the odorless carrier gas. The stimulation paradigm was 9 s of stimulus (ON period) followed by 51 s of odorless carrier gas (OFF period), with the whole ON/OFF period being repeated three times (3 min). The stimuli and odorless carrier gas were delivered as humidified after bubbling in distilled water at a flow rate of 500 mL/min. After each fMRI scanning, the subject was asked to name the odor and describe the intensity and pleasantness/unpleasantness. The answers were considered to sort the samples into the pleasant or unpleasant aroma group. The samples were presented to each subject four times, always in different sessions. Each session included a blank sample (sample vial was kept empty) to control the artifacts and activations not due to olfactory stimulation.

Acquisition of Functional Images by fMRI. The fMRI images were acquired on a General Electric 1.5 T Signa Infinity with Excite technology (General Electric Medical Systems, Madrid, Spain), equipped with echo planar capabilities using an eight-channel head coil.

An independent sequence of T2 axial scans were acquired at the beginning of each session to be used as localizer of the functional images and to rule out brain abnormalities. The functional images were acquired with gradient-echo T2*-weighted echoplanar images (EPIs) with blood oxygen level-dependent (BOLD) contrast. Imaging parameters were as follows: repetition time (TR) = 3000 ms, echo time (TE) = 35 ms, flip angle = 90°. Five dummy scans (15 s, TR = 3 s) were acquired prior to acquiring the functional images to ensure a steady state before data were collected.

The volume of the whole three-dimensional (3D) brain images was divided into small volume units (voxels). The spatial resolution was set at a 64 × 64 voxel matrix covering a 250 × 250 mm^2 field of view (FOV), a slice thickness of 4 mm with no gap, and an in-plane resolution of 3.91 × 3.91 mm^2. In each volume, 38 slices were acquired, covering the whole brain with an anterior commissure to posterior commissure (AC−PC) slice orientation. High-resolution (0.94 × 0.94 × 1.00 mm) coronal T1-weighted anatomical scans were acquired after functional scanning. The images were coregistered to the functional EPI, normalized, and averaged across subjects to aid localization.

Image Preprocessing and Statistical Analysis. The fMRI output images were divided between structural images (high-resolution images showing anatomical structures) and functional images (images containing information of brain activity). Both kinds of fMRI images were processed with SPM8 (Wellcome Department of Cognitive Neurology, London, U.K.)[6] to avoid intersubject and intersample variability and to localize the anatomical parts with activations that are correlated to the stimuli (Figure 2). Functional and structural images were reoriented in the same direction before preprocessing. Afterward, the images were subjected to a slice timing correction to obtain identical time points for all slices of a given volume. Then, images were realigned for motion correction, and they were coregistered to align functional and structural data. After the resulting images were smoothed, they were normalized to the Montreal Neurological Institute (MNI) space defined by Talairach and Tournoux,[25] which allows for associating *x*, *y*, and *z* coordinates with specific anatomical areas in the brain. The normalization process included the reslicing of the structural and functional images into 91 slices with isotropic voxel dimensions (2 mm in the three orientations). The normalized images were smoothed and submitted to statistical analysis.

The images were studied with the statistical tool based on general linear models[6] that is available in SPM8 software to find brain areas with significant activations correlated with the stimuli. The task-induced effect was identified with linear contrast of the parameter estimates by applying one-sample *t* tests. The values at each control point (voxel) for each contrast resulted in a statistical parametric map of the corresponding *t*-statistic expressed as *Z*-scores. These values denote the intensity of brain activity in each voxel. The matrix of *Z*-scores for each voxel was then imported into Statistica 6.0 (Statsoft, Tulsa, OK) for further statistical analysis. These values were projected onto the structural images, previously normalized into the Talairach space, to identify the anatomical areas associated to each activation. A threshold of 0.05 (*p*-value) was set in all the brain mappings to select only the most significant areas and dismiss those activations that could be artifacts or not associated with the olfaction task. Anatomical identification was

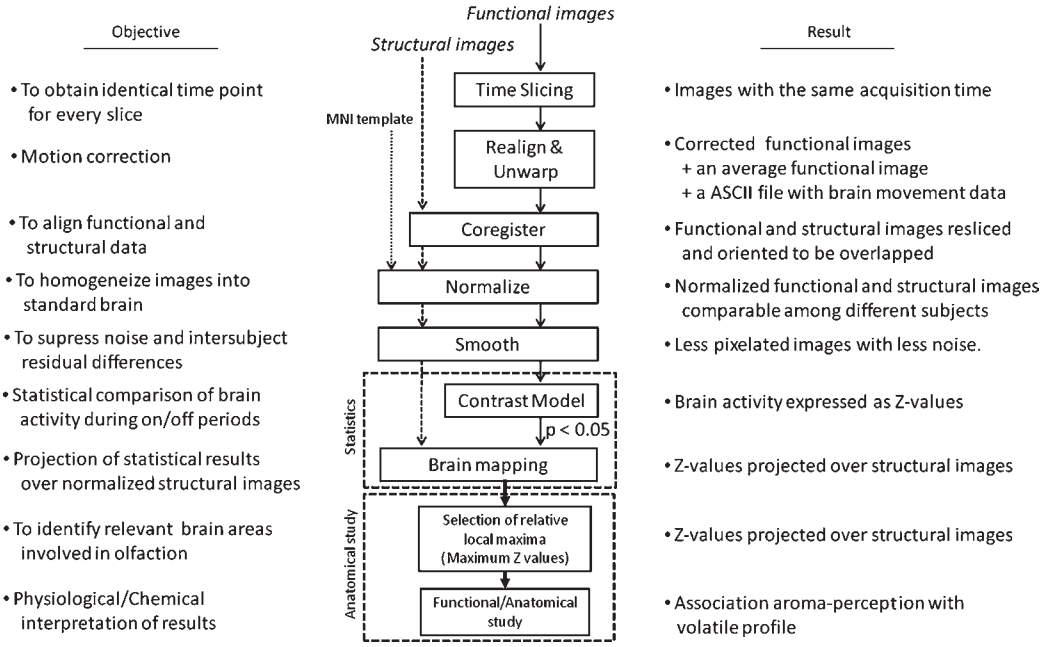

Figure 2. Steps in the processing of fMRI images. (MNI, Montreal Neurological Institute.)

Table 1. Results of the Sensory Assessment of the Samples Used in the fMRI Experiments

samples	Md[a] (% RSD)	Mf[b] (% RSD)	main sensory characteristics
EVOO cv. Royal	0 (0%)	4.5 (5.2%)	green-fruity, green-apple
EVOO cv. Arbequina	0 (0%)	4.0 (6.9%)	mature green/fruity, tomato
EVOO cv. Picual	0 (0%)	4.2 (5.7%)	green-lawn, bitter
rancid VOO	2.9 (9.8%)	0 (0%)	old peanut butter, wax crayons
fusty VOO	4.0 (10.5%)	0 (0%)	gym clothes, decomposing olives
winey VOO	7.7 (12.9%)	0 (0%)	nail polish, acetic acid, vinegar

[a] Median of defects. [b] Median of fruitiness.

assisted with Talairach Client 2.4.2 (Research Imaging Center, San Antonio, TX) to associate the Talairach coordinates (x, y, z) with specific anatomical areas. The functional meaning of the activations was interpreted by means of the organization of the brain into Brodmann areas (BA), each one being associated with diverse functions.[10] Detailed information on BAs and the associated functions can be found in ref 26.

RESULTS AND DISCUSSION

Sensory and Chemical Characterization of the Samples. The sensory assessment of virgin olive oils, although being a normalized method,[1] is partially biased by a certain subjectivity of the judgments given by the panelists. The samples under study were subjected to a sensory assessment to determine the median of defects (Md) and the median of the fruity sensory attribute (Mf), thereby certifying their inclusion within the categories of extra virgin olive oil and lampante virgin olive oil (Table 1). The three extra virgin olive oils were qualified with a median of fruity attribute of 4−4.5, although with a relative standard deviation (% RSD) of 5.2−6.9%. On the other hand, the samples with sensory defects (rancid, fusty, and winey) were qualified, as expected, with a high value of Md (2.9, 4.0, and 7.7, respectively). Although all the panelists agreed about the main sensory defects of each sample, the scores given by the panelist varied with a % RSD up to 12.9%, which points out the difficulty in reaching a consensus on the perceived intensity. This high % RSD is partly due to the biased sensitivity of some panelists to some defects over others, which justifies the necessity of analyzing volatile compounds to obtain objective information about the aroma, which is free of the panelist's conditioning.

The volatile compounds quantified in the samples are presented in Table 2, together with the odor thresholds and the sensory characteristics. The odor activity value (OAV) of each compound, expressed as the ratio between the concentration and the odor threshold, revealed that 17 volatile compounds contribute to the aroma of extra virgin olive oil (OAV > 1). Among them, compounds remarkable for having high OAV and contributing with pleasant sensory attributes are 3-methyl-butanal, pentanal, 1-penten-3-one, hexanal, *E*-2-hexenal, and *Z*-3-hexen-1-ol. Most of these compounds are characterized with fruity, sweet, and green aromas, although some of them (mainly hexanal, hexanol, and *E*-2-heptenal) are also responsible for unpleasant attributes when they are present at high concentrations.[22,23,27] Some compounds contributing to unpleasant attributes (2,4-hexadienal, *E*-2-decenal, and butanoic and hexanoic acids) were quantified at concentrations higher than their corresponding odor thresholds. These compounds were probably masked by the rest of the odorants, and they were not perceived by the panelists because no one reported sensory defects in these samples. The occurrence of these compounds in extra virgin olive oil points out the importance of the masking effect between volatiles and the necessity of considering the whole volatile profile for an accurate sensory interpretation. This masking effect is less significant in lampante virgin olive oils, where the account of volatile compounds contributing with unpleasant attributes

Table 2. Concentration of Volatile Compounds (mg/kg) Quantified in Six Virgin Olive Oils of the Categories Extra Virgin (EVOO[a]) and Lampante (LVOO[b]), together with Sensory Descriptors and Odor Thresholds (OT)

volatile compound	Trr[c]	Kovats index	LVOO mean ± STD	EVOO mean ± STD	sensory descriptors	OT
octane	0.19	800	16.27 ± 5.59	0.55 ± 0.31	alkane, solvent	0.94
methyl acetate	0.20	828	0.92 ± 0.41	0.27 ± 0.12	sweet, ethereal	0.20
E-2-octene	0.23	830	0.20 ± 0.11	tr[d]	plastic	8.75
butanal	0.25	832	tr[d]	0.09 ± 0.04	green, pungent	0.15
ethyl acetate	0.26	892	17.57 ± 16.41	0.51 ± 0.12	sticky, sweet, aromatic	0.94
3-methyl butanal	0.29	910	tr[d]	0.04 ± 0.03	sweet, fruity, ripe fruit, almond	0.0054
ethanol	0.31	932	6.71 ± 2.16	36.80 ± 26.54	apple, sweet, alcohol	30.00
ethyl propionate	0.35	950	0.72 ± 0.40	0.09 ± 0.04	fruity, strawberry, apple, sweet	0.10
pentanal	0.38	969	1.34 ± 0.66	1.15 ± 0.95	oily, wood, bitter, almond	0.24
4-methyl-2-pentanone	0.44	980	tr[d]	0.24 ± 0.24	fruity, strawberry, sweet	0.30
1-penten-3-one	0.47	1016	tr[d]	0.28 ± 0.16	pungent, mustard	0.0007
2-butanol	0.50	1024	1.81 ± 0.99	0.07 ± 0.03	winey	0.15
hexanal	0.67	1074	10.88 ± 6.85	2.14 ± 0.19	oily, fatty, green, green apple, lawn	0.80
2-methyl-1-propanol	0.72	1099	tr[d]	0.02 ± 0.01	solvent, penetrating, wine, butter	1.00
E-2-pentenal	0.82	1131	3.19 ± 1.53	0.50 ± 0.16	harsh green, apple, tomato, pungent	0.30
1-butanol	0.92	1145	0.02 ± 0.01	0.03 ± 0.01	sickly sweet, oily, medicine	
2-heptanone	1.02	1170	1.15 ± 1.03	tr[d]	watered earth, soap, cinnamon	0.30
heptanal	1.03	1174	6.87 ± 6.27	0.16 ± 0.08	greasy, rancid	0.50
limonene	1.09	1201	0.08 ± 0.04	0.03 ± 0.02	citrus, mint	
3-methyl-1-butanol	1.13	1213	0.20 ± 0.17	0.18 ± 0.11	whiskey, woody, burnt, unpleasant, sweet	0.10
E-2-hexenal	1.14	1216	2.07 ± 0.70	25.49 ± 18.01	bitter almond, fruity, green	0.42
3-octanone	1.26	1244	0.84 ± 0.61	1.77 ± 0.77	grass, mold, green, butter	
hexyl acetate	1.29	1274	0.11 ± 0.07	0.02 ± 0.01	sweet, fruity, apple, green grass	1.04
2-octanone	1.35	1279	1.90 ± 1.58	0.05 ± 0.03	mold, over ripe, fruity	0.50
octanal	1.36	1280	44.91 ± 44.16	0.37 ± 0.22	greasy, soap, fatty	0.32
E-2-heptenal	1.46	1282	18.21 ± 17.41	2.61 ± 1.44	soap, greasy, almond, pungent	0.005
2-heptanol	1.48	1288	0.45 ± 0.42	0.43 ± 0.27	mushroom, earthy, sweet	0.01
Z-2-pentenol	1.50	1320	0.02 ± 0.01	0.09 ± 0.04	banana	0.25
6-methyl-5-hepten-3-one	1.51	1347	0.42 ± 0.21	0.07 ± 0.04	fruity, green, grass, pungent	1.00
hexanol	1.57	1357	0.54 ± 0.24	3.58 ± 1.31	fruity, sweet, aromatic	0.40
E-3-hexen-1-ol	1.61	1366	0.05 ± 0.03	0.02 ± 0.01	green lawn	1.00
Z-3-hexen-1-ol	1.65	1378	0.54 ± 0.51	2.49 ± 1.50	banana, fresh, green lawn	1.10
nonanal	1.66	1385	481.99 ± 470.76	4.78 ± 1.77	rancid, fatty, waxy, pungent	0.15
2,4-hexadienal	1.68	1391	60.01 ± 37.00	15.60 ± 7.92	fresh, green, floral, citric	0.27
acetic acid	1.73	1450	35.09 ± 23.21	3.69 ± 1.95	sour, vinegary	0.50
2,4-octadienal	2.09	1555	0.92 ± 0.63	0.05 ± 0.03	green, seaweed	1.00
2-methylpropanoic acid	2.12	1563	8.13 ± 7.14	tr[d]	rancid, buttery, cheese	
butanoic acid	2.26	1628	26.57 ± 23.51	1.43 ± 1.24	rancid, fusty, cheese	0.65
E-2-decenal	2.28	1651	38.00 ± 36.55	1.82 ± 1.14	tallow, painty, fishy, fatty	0.01
pentanoic acid	2.50	1720	14.71 ± 8.57	0.25 ± 0.13	rancid, unpleasant, pungent	0.60
E-2-undecenal	2.52	1760	457.81 ± 436.19	tr[d]	soap, grease, green	4.20
hexanoic acid	2.73	1829	113.40 ± 102.36	1.98 ± 0.69	rancid, sour, sharp	0.70
heptanoic acid	2.94	1990	1.42 ± 1.15	0.03 ± 0.01	rancid, fatty	0.10
octanoic acid	3.15	2083	122.43 ± 80.94	3.27 ± 0.90	rancid, cheese, oily, fatty	3.00
nonanoic acid	3.35	2202	0.86 ± 0.45	0.12 ± 0.04	grease, green	

[a] Cultivar Royal, Arbequina, and Picual. [b] Rancid, fusty, and winey-vinegary defects. [c] Trr, relative retention time. [d] tr, trace levels.

counterbalance or exceed the number of compounds responsible for green-fruity attributes, which is undoubtedly reflected in the sensory assessment given by panelists. Thus, in general terms, remarkable compounds producing negative perceptions are some aldehydes, such as hexanal (responsible for a fatty perception at high concentration),[22,23] heptanal, octanal, *E*-2-heptenal, nonanal, *E*-2-decenal, and *E*-2-undecenal, together with some alcohols (e.g., 2-butanol), ketones (e.g., 2-octanone), and all the organic acids. Nevertheless, the most significant volatile compounds contributing to the negative perceptions depend on the kind of defect, which is reflected in a major variance between the defective samples compared to extra virgin olive oils and a high

Table 3. Sensory Perception Described by Three Panelists (Attributes Selected under Consensus) of Three Concentrations of Hexanal in Refined Oil, Smelled through the Olfactometer at Different Flow Rates

		hexanal		
flow (mL/min)	rancid oil	35 mg/kg	100 mg/kg	200 mg/kg
100	rancid-green	fresh, slightly rancid	green-lawn	sweet-green
200	rancid-green	fresh, slightly rancid	green-fatty	intense green-rancid
400	rancid	fresh-rancid	rancid	rancid-pungent
600	rancid	rancid	green-rancid	rancid-fatty
800	slightly rancid	rancid	green-rancid	rancid-green
1000	rancid-green	fresh-rancid	green-rancid	green-rancid
no flow (directly smelled from vial)	rancid	fresh, slightly rancid	rancid	rancid, pungent, strong

standard error of the mean (Table 2). Thus, high concentrations of aldehydes were particularly remarkable in the rancid oil, as a consequence of oxidation:[23] hexanal (31.36 mg/kg), heptanal (25.67 mg/kg), *E*-2-heptenal (70.43 mg/kg), octanal (177.37 mg/kg), nonanal (1894.21 mg/kg), 2,4-hexadienal (11.38 mg/kg), *E*-2-decenal (147.60 mg/kg), and *E*-2-undecenal (57.89 mg/kg). The rancid oil also shows the highest concentrations of hexanoic and octanoic acids (420.19 and 364.76 mg/kg, respectively). The odor thresholds for these compounds prove that the panelists perceived their aroma in the rancid oil and these compounds greatly determined the high score of the median of defects. Likewise, the median of defects given to the winey oil was greatly due to the high concentration of acetic acid (102.12 mg/kg) and ethyl acetate (66.80 mg/kg), which agrees with previous results characterizing this sensory defect.[23,28] The fusty oil was characterized with high concentrations of some aldehydes such as nonanal (14.96 mg/kg) and, overall, for the high concentration of acids, such as butanoic (96.83 mg/kg), pentanoic (23.98 mg/kg), hexanoic (23.54 mg/kg), and octanoic acids (48.26 mg/kg). Both aldehydes and acids originate from the fermentation process of the olives before milling,[23] which resulted in the unpleasant fusty perception described by the panelists. The high concentration of all these compounds responsible for the sensory defects explained the fact that no panelist disagreed in the description of the defects, and only the intensity (median of defects) was the parameter under discussion.

Optimization of fMRI Experiments. The study of the olfactory perception that results when a panelist or consumer smells virgin olive oil aroma involves presenting the volatile compounds at the same conditions as in a real situation. This is one of the requirements for the development of new analytical methods for flavor analysis of virgin olive oil,[29] and likewise it was also considered for the design of a new odorant delivery system for the fMRI studies. Thus, the olfactometer design was inspired by the systems for electronic noses consisting of tubes and valves.[4] After several designs were tested, the scheme shown in Figure 1 was finally selected to place the valve that switched between clean and odorant streams as close to the nasal mask as possible. Such a design avoids cross-contamination between functional runs and ensures an odorless clean carrier gas in the off periods. As no metallic items are allowed in the magnetic room because they interfere in the measurements, a small three-way valve (25 g) made mostly of PTFE and PVC was selected. The metallic part and the working voltage (24 V) produced no artifacts in the measurements as was demonstrated during phantom scanning (examining an anthropomorphic object to test the performance of the magnetic resonance imaging system). All connecting tubes, nuts, ferrules, and pluggings were made of Teflon because other materials such as silicon or plastic absorb aromas and cause cross-contamination between samples.

Once the olfactometer was designed, the main parameter to be optimized was the carrier gas flow rate. This parameter was optimized considering three factors: (i) the speed in delivering the odorant and the delay in perceiving the olfactory stimuli; (ii) the description of the perception given by the subject, which is greatly modified by the flow rate; and (iii) the comfort in receiving a streamflow within the nostrils for more than 30 min (dry feeling, irritation of mucosa). The flow rate was optimized within the range 100−1000 mL/min: 100 mL/min being the flow rate that is commonly used in headspace sampling in electronic nose and chromatographic analyses[4] and 1000 mL/min being the maximum flow rate provided by the carrier gas source. The delay in the odorant delivery also depends on the tube length. Once the tubes were shortened up to the minimum length, determined by the safety distance between the valve and the fMRI scanner, a delay in the perception of 1.5 s or shorter was considered appropriate, given that the scanning period (TR) of the fMRI instrument was 3 s.

Concerning the sensory perception described by the subjects during the aroma delivery, it was observed that the perception of rancid aromas was greatly modified by the flow rate because of a dilution effect of the gas stream on the concentration of volatile compounds. Thus, some subjects reported a pleasant fresh and green aroma when they smelled rancid oils from the olfactometer, whereas they described the aroma as unpleasant when it was smelled from the vial. The variation in the perception of rancid oils is due to the different sensory descriptors of hexanal at low (fresh aroma) and high (rancid and fatty) concentrations.[22] Thus, the original concentration of hexanal in the headspace of the rancid oil (Table 2) decreased when this compound was diluted in the gas stream, and consequently it provided a different perception. In consequence, the optimization of the flow rate was carried out by testing a rancid oil and three dilutions of hexanal in refined oils at 35 ppm, 100 ppm, and 200 ppm, delivered by the olfactometer and smelled by three assessors. A flow rate higher than 600 mL/min provided a pleasant fresh aroma even at the highest concentrations of hexanal due to the dilution effect, while lower flow rates were able to reproduce the perception of the aromas as smelled from the vial (Table 3). The suitability of flow rates lower than 600 mL/min in not modifying the sensory perception of the samples was later checked with all the virgin olive oil samples.

Finally, the comfort of smelling the aromas delivered from the olfactometer limited the flow rate to values lower than 500 mL/min,

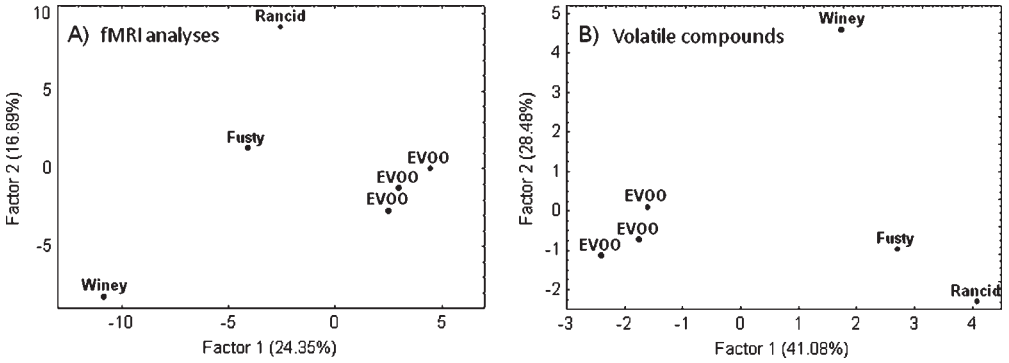

Figure 3. PCA plot obtained from the whole data set of fMRI scanning (A) and volatile concentrations (B) for six samples of virgin olive oil presented to one subject (EVOO, extra-virgin olive oil).

as a higher flow produced nasal irritation. Thus, considering a range of 100−500 mL/min, the optimum flow rate was selected by applying a modified Simplex procedure,[30] which was completed after running six tests with three subjects who reported the suitability of the flow rate in terms of the speed in producing the olfactory perception, comfort, and odor habituation. This procedure selected an optimum flow rate of 450 mL/min, as it allows for a short perception delay (no longer than 1 s) and does not modify the sensory perception of the odorant via the dilution effect.

Under this flow rate, the valve controller was adjusted to test three stimulation paradigms: 3 s (aroma)/57 s (rinse); 9 s (aroma)/51 s (rinse); and 15 s (aroma)/45 s (rinse). The best paradigm was selected on the basis of the statistical value of the brain activation in the primary olfactory cortex (POC), orbitofrontal, and temporal activation areas that are related to the olfaction process and consequently should be activated during the olfactory task.[12] Therefore, it is expected that the activation in this region shows a high level of statistical significance in their correlation to the stimulus, regardless of the type of odor that is presented. The statistical significance value (Z) found in entorhinal cortex (within the POC) determined that the paradigm 9 s (aroma)/ 51 s (rinse) provided the best correlation with the stimuli ($Z > 5$ for $p < 0.05$ in most cases). The selection of an on period of 9 s to present the aroma agrees with previous fMRI studies carried out on olfactory tasks.[31] Furthermore, this paradigm offered the advantages of rapid rinses after the stimuli and a high perception intensity during the onset periods, with almost no odor habituation, which would explain the higher statistical significance values found in both the primary and secondary olfactory cortices compared with the other two paradigms.

fMRI Analyses. The selected stimulation paradigm was applied to present the aromas of virgin olive oils to the subjects during the fMRI experiments. The onset/offset periods specified in the SPM software were based on the actual perception rather than the open/close valve times because some authors have found that the correlation based on sensory perception allows for detecting activation at a higher statistical significance compared with the predefined onset/offset times.[12,32] Although the open/close valve times matched with the perception periods in most cases, three assessors tested the aromas along the selected paradigm prior to fMRI experiences, and they described the temporal evolution of the olfaction perception. Only in the case of samples characterized with a strong odor (e.g., fusty virgin olive oils) did the onset/offset periods programmed in the valve controller differ from the actual perception periods, and the latter were then considered in the SPM software.

For the data analysis, the 3D data matrix obtained from each fMRI experience was unfolded into a two-dimensional matrix by using MATLAB, and it was subsequently submitted to statistical analysis. A principal component analysis (PCA) plot (Figure 3A) of those voxels with Z-values different from zero showed that the variance within the samples for a single subject is, to some extent, related to the kind of aroma. Thus, the aromas of extra virgin olive oils (EVOO) were located at positive values of factor 1 and close to zero for factor 2. On the contrary, defective samples (fusty, rancid, and winey oils) were located at negative values of factor 1. Considering that the brain activations and the consequent sensory perceptions are the result of smelling all the volatile compounds as a whole, a PCA was similarly carried out with the whole data set of volatile concentrations (Table 2) to establish the differences between samples according to their complete volatile composition. The PCA plot (Figure 3B) showed clear differences between lampante virgin olive oils and the extra virgin olive oils due to qualitative differences in volatile composition (Table 2), which was also observed in Figure 3A for fMRI analyses. In both PCAs, it was observed that the dispersion of extra virgin olive oil samples was lower compared to lampante olive oil because of the higher differences in the volatile profile of defective samples. Although factor 1 allowed the separation of pleasant and unpleasant samples in both PCAs, the explained variance was higher in volatile analyses than in the fMRI analyses (41.08 vs 28.35%). The lower explained variance for fMRI analyses can be due to the effect of the differences between individuals and unknown factors in perception in comparison with the highly objective information provided by chemical analysis of volatile compounds.

The high variability between the samples observed in the PCA plots of each subject individually analyzed pointed out the importance of some anatomical zones over others in distinguishing pleasant and unpleasant odors.[33] Consequently, the study of all the data by PCA, examined as a whole, was followed by the identification of specific anatomical zones with significant activations in samples characterized by sensory defects compared with virgin olive oils.

As a preliminary study, the identification of the brain activities was centered on those slices that showed the highest activations in most of the samples. For this purpose, the exported data (Z-values) in the unfolded files were examined to search for the highest values of activations. The corresponding slices (planar images) showing these high Z-values were selected to carry out a comparative study of the samples. A fixed pattern was observed in the selected slices and in the groups of voxels (small volume

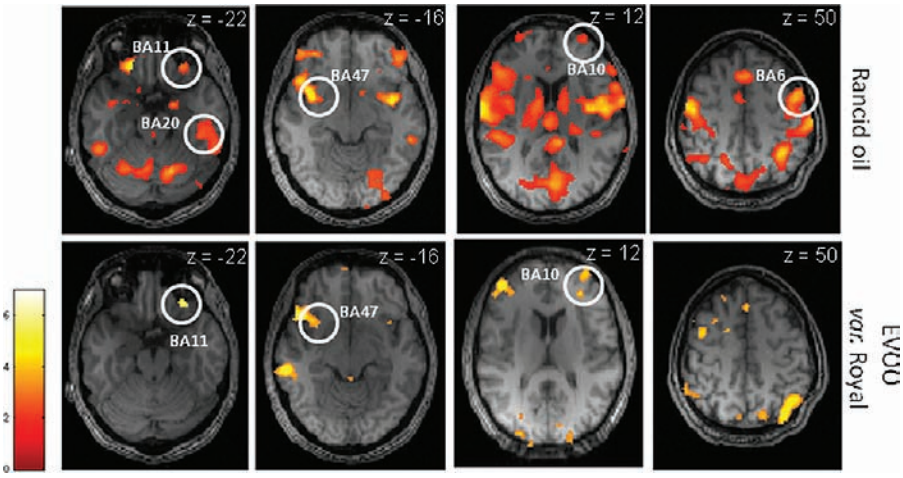

Figure 4. Axial activations ($p < 0.05$) in response to the aromas of an extra virgin olive oil var. Royal (EVOO) and a rancid virgin olive oil. Brodmann areas (BA) 6, 10, 11, 20, and 47 are marked with circles. The third Talairach coordinate (z) is shown on each image.

Table 4. Summary of Brain Activations Determined by fMRI During Olfaction of Virgin Olive Oil Aroma

BA[a]	ROI[b]	hemisphere[c]	Talairach coordinates (x, y, z)	z-score ($p < 0.05$)	comment
6	frontal lobe, middle frontal gyrus	R, L, or R/L	42, 4, 50	4.51	Activated in most unpleasant samples and some fragrant pleasant ones.
9	prefrontal cortex−middle frontal gyrus	L/R	−54, 22, 24	4.69	
10	frontal lobe, superior frontal gyrus	R or L/R	30, 60, 12	2.31	Activated in most of the samples.
11	frontal lobe, inferior frontal gyrus	L/R	−22, 34, −22	4.76	Active in unpleasant aromas.
13	sublobar, insula	R	32, 18, 10	2.27	Occasionally activated, mostly in unpleasant oils.
20	temporal lobe, inferior temporal gyrus	L/R or R	60, −38, −23	3.26	
24, 32, 33	limbic lobe, cingulate gyrus	L/R	−2, 18, 38	1.99	Much more activated in unpleasant aromas. The voxels of the three areas are commonly overlapped.
38	temporal lobe, superior temporal gyrus	L or L/R	−40, 16, −28	3.70	Activated in unpleasant aromas.
40	parietal lobe, inferior parietal lobule	L/R	−50, −38, 28	5.22	
47	frontal lobe, inferior frontal gyrus	L or L/R	−20, 16, −16	4.27	Bilaterality is mostly shown in unpleasant samples.

[a] Brodmann area. [b] Region of interest. [c] R, right hemisphere, L, left hemisphere.

units) that are repeatedly activated by the pleasant and unpleasant aromas. Thus, most of the pleasant samples showed the highest activations around four slices (coordinate z = −43.9, −25.5, −2.2, and 54.5 in the normalized brain). In the samples characterized by unpleasant aromas, the higher values were also identified in four slices (z = −55.6, −18.9, −0.5, and 22.8). In this case, the variability between samples was much higher, and high values of activations were also observed in many other slices, which agrees with the location of the samples in Figure 3A,B. The high variation in the defective samples also corresponds to the high standard error of the mean that was calculated for most of the volatile compounds that were quantified in these samples, in comparison with extra virgin olive oils (Table 2). The identification of the anatomical zones activated by the odor stimuli was started on the selected slices mentioned above and continued with the surrounding areas. The representative voxel groups were interpreted according to the anatomical zone, verified by the Talairach coordinates. The coordinates submitted to the anatomy atlas (Talairach Client 2.4.2) were those where the nearest local maximum (Z-value) was registered.

In all the fMRI experiences, high activation values were registered in the orbitofrontal, frontal, and temporal lobes. These zones corresponded to the Brodmann areas 10, 11, and 20 (Figure 4). Bilateral activations on BA 10 and 11 were associated to the olfaction process itself,[34,35] which explains their activation in response to both pleasant and unpleasant samples regardless of their volatile compounds. An increment in cerebral blood flow at BA 11 (Table 4) is also associated with the familiarity of the odors, which would explain the high intensities observed in subjects that were regular consumers of virgin olive oils. The recognition of those aromas is ultimately related to the occurrence of C5 and C6 volatile compounds that normally are present in good quality virgin olive oil (Table 2).

In most cases, an activation in the inferior temporal lobe (BA 20) was also found (Figure 4). This activation was bilateral in some odors, while in the others only one side (right side) was activated. The activation of this area has been related to recognition and working memory tasks,[36] probably associated with the consumption habits of the subjects. It is important to note that subjects were asked to name the odors after the fMRI experiences, so it may cause the activation of those areas related to memory retrieval and naming. On the other hand, although fusty and winey aromas might be unknown odors to the subjects, rancid odors are among the most well-known unpleasant aromas.

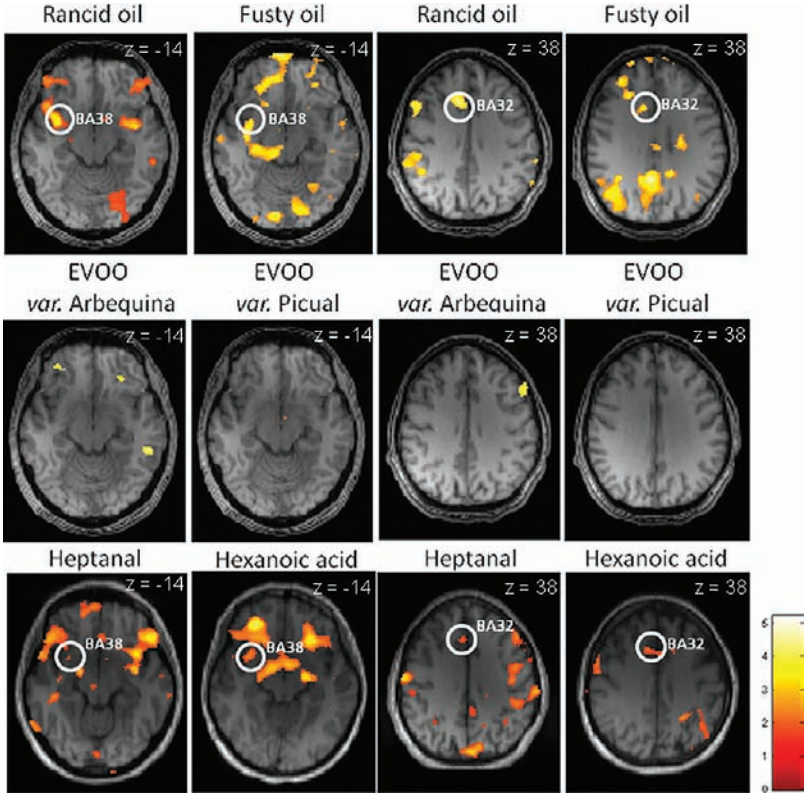

Figure 5. Axial activations ($p < 0.05$) in response to the aromas of extra virgin olive oil (EVOO) and virgin olive oils with sensory defects. Brodmann areas (BA) 32 and 38 are marked with circles. The third Talairach coordinate (z) is shown on each image.

Thus, people are commonly familiarized with the rancid odor produced by a rise in hexanal and other aldehydes originating from oxidation (Table 2), and this defect may evoke negative memories of them.

The importance of memory integration and recognition tasks in the olfaction process was also pointed out by the maximum responses to pleasant odors. In the olfaction of pleasant aromas of virgin olive oils, characterized by positive green and fruity aromas (due to the presence of volatiles such as *E*-2-hexenal, hexanal at low concentration, and *Z*-3-hexen-1-ol, among many others), the maximum responses were mostly localized in the inferior frontal gyrus, BA 47 (Figure 4). The activation of this area is also related to the recognition of familiar odors.[37] On the contrary, the maximal responses recorded for unpleasant odors (rancid, fusty, and winey virgin olive oils) corresponded with the inferior parietal lobule in the assigned BA 40, which is bilaterally activated. This area is activated during aversive feelings,[38] which would explain its activation during smelling of off-flavors in defective virgin olive oil. This negative perception is due to the volatile compounds quantified at a high concentration in these samples, mainly aldehydes and acids that have low odor thresholds (Table 2). No activation in this area was observed when smelling good quality virgin olive oils, where these compounds were not present or they were present at low concentration (e.g., acids).

Other areas related to negative feelings were activated in most of the unpleasant aromas, with no activation in pleasant samples. Thus, the temporal gyrus was activated in BA 38 in the left side or bilaterally (Table 4, Figure 5). This activation could point out aversion or dislike, according to previous studies that have related this area to negative emotions.[39]

Intense activations were also found in the Brodmann areas numbered 24, 32, and 33 when virgin olive oils with off-flavors were presented to the subjects. Those activations in the anterior cingulated gyrus (Table 4) during the presentation of defective virgin olive oils seem to be related to aversiveness and negative emotions. Again, this perception is produced by those volatiles that are present in defective oils at high concentrations (Table 1) because no activation is observed in EVOOs. Thus, Fulbright et al.[40] detected significant activation in BA 32 (lateralized to left) in response to a compound responsible for an unpleasant aroma (isovaleraldehyde). In order to check the hypothesis that the activation of the cingulate area in the BA 32 was due to an unpleasant perception, two volatile compounds characterized by undesirable aromas, heptanal and hexanoic acid, were presented to subjects. These compounds were diluted in odorless refined oil at 100 mg/kg. Both volatiles are produced during oxidation and fermentation processes, and they are commonly present in virgin olive oils with sensory defects.[23] The concentrations quantified in the defective samples for these compounds were higher than their odor thresholds (Table 2), and in consequence, they contributed to the aroma perceived by the panelists. In particular, the contribution of heptanal to the rancid aroma of oils is significant, with saturated aldehydes, originating during the oil oxidation process, being mainly responsible for the rancid and fatty sensory descriptors.[23] On the other hand, hexanoic acid was the most abundant organic acid in all the defective samples, and its concentration was up to 200 times higher in defective oils compared to extra virgin olive oils (Table 2). During the fMRI experiments, all the subjects described the aroma of the dilution of these compounds as unpleasant and an intense activation was observed in BA 32 (Figure 5). A high activation was also detected

in BA 38, as it was previously observed in defective virgin olive oil samples.

In addition to areas that are activated in response to off-flavors, other brain areas act as modulators in the cognitive processing of odors, although they are not activated consistently in all the samples. Thus, strong odors (both pleasant and unpleasant) elicited an intense activation in BA 6 (Figure 4). In most cases, the activation in this area was observed in the defective samples (e.g., rancid and fusty oils) and in a good quality sample characterized by an intense green-fruity aroma (Arbequina virgin olive oil). Thus, Table 2 shows that 26 volatile compounds in defective samples have concentrations exceeding their odor threshold, compared to only 17 compounds in extra virgin olive oil. The activation of this area in the left hemisphere is associated with strong odors, as was reported by Miyanari et al.,[41] who did not observe activation when weak odorants were presented to the subjects. Thus, the activation in this area may modulate the pleasantness of the aroma, because the perceived intensity has an important role in rising/diminishing pleasantness.

The results obtained after presenting the aroma of pleasant and unpleasant virgin olive oils show that the hedonic valence of olfactory perception is explained by the combinatory effect of three groups of brain areas. First, some of them (BA 9, 10, 11, 13, 20, and 47) are activated in both pleasant and unpleasant samples, and their activation is clearly related to the olfaction process itself. A second group of BAs (mainly 32 and 38) points out aversiveness, and they are activated in most of the unpleasant samples. Finally, the third group of brain areas act as modulators of the perception, indicating the strength of the aroma (BA 6) and familiarity (BA 9, 40, and 47). To our knowledge, no previous fMRI study has been focused on the aroma of extra virgin olive oil. The results are being checked with more individuals, more kinds of oils, and more volatile compounds. On the other hand, the implementation of postreceptor studies by brain imaging to interpret sensory perception could also be improved by devising new procedures of data normalization to avoid between-day variations in the sensitivity of the fMRI instrument. The between-day variation is not corrected by the described image normalization (Figure 2), and an additional normalization of functional data would allow a higher confidence level (p-value) with better repeatability and robustness in the results. The information resulting from this research will help in understanding consumer preferences for some particular varieties of virgin olive oils, integrating multimodal features of oil perception such as taste (bitterness, pungency, astringency) and color.[19] Furthermore, an improved procedure for fMRI would allow determining the volatile compounds responsible for sensory defects according to physiological evidence in addition to sensory fundamentals.

AUTHOR INFORMATION

Corresponding Author

*Tel: +34954611550. Fax: +34954616790. E-mail: dluisg@cica.es.

Funding Sources

This research has been funded by the Spanish Ministry of Science and Innovation (Project AGL2008-01411).

REFERENCES

(1) *Organoleptic Assessment of Virgin Olive Oil*; International Olive Council: Madrid, Spain, 1996; COI/T.20/ Doc. No. 15 Rev. 1.

(2) Escuderos, M. E.; Uceda, M.; Sánchez, S.; Jiménez, A. Instrumental technique evolution for olive oil sensory analysis. *Eur. J. Lipid Sci. Technol.* **2007**, *109*, 536–546.

(3) Vichi, S.; Guadayol, J. M.; Caixach, J.; López-Tamames, E.; Buxaderas, S. Comparative study of different extraction techniques for the analysis of virgin olive oil aroma. *Food Chem.* **2007**, *105*, 1171–1178.

(4) García-González, D. L.; Aparicio, R. Coupling MOS sensors and gas chromatography to interpret the sensor responses to complex food aroma: Application to virgin olive oil. *Food Chem.* **2010**, *120*, 572–579.

(5) Faurion, A.; Kobayakawa, T.; Cerf-Ducastel, B. Functional magnetic resonance imaging study of taste. In *The Senses: A Comprehensive Reference. Vol. 4: Olfaction and Taste*; Firestein, S., Beauchamp, G. K., Eds.; Academic Press: San Diego, CA, 2008; pp 271−279.

(6) Friston, K. Statistical parametric mapping. In *Statistical Parametric Mapping: The Analysis of Functional Brain Images*; Penny, W. D., Friston, K. J., Ashburner, J. T., Kiebel, S. J., Nichols, T. E., Eds.; Academic Press: London, U.K., 2007; pp 10−31.

(7) Bifone, A.; Gozzi, A.; Schwarz, A. J. Functional connectivity in the rat brain: A complex network approach. *Magn. Reson. Imaging* **2010**, *28*, 1200–1209.

(8) Tabert, M. H.; Steffener, J.; Albers, M. W.; Kern, D. W.; Michael, M.; Tang, H.; Brown, T. R.; Devanand, D. P. Validation and optimization of statistical approaches for modeling odorant-induced fMRI signal changes in olfactory-related brain areas. *NeuroImage* **2007**, *34*, 1375–1390.

(9) Cerf-Ducastel, B.; Murphy, C. Validation of a stimulation protocol suited to the investigation of odor-taste interactions with fMRI. *Physiol. Behav.* **2004**, *81*, 389–396.

(10) Marciani, L.; Eldeghaidy, S.; Spiller, R. C.; Gowland, P. A.; Francis, S. T. Brain imaging. In *Food Flavour Technology*; Taylor, A. J., Linforth, S. T., Eds.; Wiley: Oxford, U.K., 2010; pp 319−350.

(11) Cox, R. W. AFNI: Software for analysis and visualization of functional magnetic resonance neuroimages. *Comput. Biomed. Res.* **1996**, *29*, 162–173.

(12) Cerf-Ducastel, B.; Murphy, C. fMRI activation in response to odorants orally delivered in aqueous solutions. *Chem. Senses* **2001**, *26*, 625–637.

(13) Qureshy, A.; Kawashima, R.; Imran, M. B.; Sugiura, M.; Goto, R.; Okada, K. E. N.; Inoue, K.; Itoh, M.; Schormann, T.; Zilles, K.; Fukuda, H. Functional mapping of human brain in olfactory processing: A PET study. *J. Neurophysiol.* **2000**, *84*, 1656–1666.

(14) Marciani, L.; Pfeiffer, J. C.; Hort, J.; Head, K.; Bush, D.; Taylor, A. J.; Spiller, R. C.; Francis, S.; Gowland, P. A. Improved methods for fMRI studies of combined taste and aroma stimuli. *J. Neurosci. Methods* **2006**, *158*, 186–194.

(15) Cerf-Ducastel, B.; Murphy, C. FMRI brain activation in response to odors is reduced in primary olfactory areas of elderly subjects. *Brain Res.* **2003**, *986*, 39–53.

(16) Francis, S.; Rolls, E. T.; Bowtell, R.; McGlone, F.; O'Doherty, J.; Browning, A.; Clare, S.; Smith, E. The representation of pleasant touch in the brain and its relationship with taste and olfactory areas. *NeuroReport* **1999**, *10*, 453–459.

(17) Rolls, E. T.; Kringelbach, M. L.; De Araujo, I. E. Different representations of pleasant and unpleasant odours in the human brain. *Eur. J. Neurosci.* **2003**, *18*, 695–703.

(18) Savic, I.; Gulyas, B.; Larsson, M.; Roland, P. Olfactory functions are mediated by parallel and hierarchical processing. *Neuron* **2000**, *26*, 735–745.

(19) Verhagen, J. V.; Engelen, L. The neurocognitive bases of human multimodal food perception: Sensory integration. *Neurosci. Biobehav. Rev.* **2006**, *30*, 613–650.

(20) Royet, J. P.; Koenig, O.; Gregoire, M. C.; Cinotti, L.; Lavenne, F.; Le Bars, D.; Costes, N.; Vigouroux, M.; Farget, V.; Sicard, G.; Holley, A.; Mauguière, F.; Comar, D.; Froment, J. C. Functional anatomy of perceptual and semantic processing for odors. *J. Cognit. Neurosci.* **1999**, *11*, 94–109.

(21) Royet, J. P.; Plailly, J.; Delon-Martin, C.; Kareken, D. A.; Segebarth, C. fMRI of emotional responses to odors: Influence of hedonic valence and judgment, handedness, and gender. *NeuroImage* **2003**, *20*, 713–728.

(22) Kalua, C. M.; Allen, M. S.; Bedgood, J.; Bishop, A. G.; Prenzler, P. D.; Robards, K. Olive oil volatile compounds, flavour development and quality: A critical review. *Food Chem.* **2007**, *100*, 273–286.

(23) Morales, M. T.; Luna, G.; Aparicio, R. Comparative study of virgin olive oil sensory defects. *Food Chem.* **2005**, *91*, 293–301.

(24) Tena, N.; Lazzez, A.; Aparicio-Ruiz, R.; García-González, D. L. Volatile compounds characterizing Tunisian Chemlali and Chetoui virgin olive oils. *J. Agric. Food Chem.* **2007**, *55*, 7852–7858.

(25) Talairach, J.; Tournoux, P. *Co-Planar Stereotaxic Atlas of the Human Brain*; Thieme: Stuttgart, Germany, 1988.

(26) Bernal, B.; Perdomo, J. *Brodmann's Interactive Atlas*; http://www.fmriconsulting.com/brodmann/Interact.html

(27) Aparicio, R.; Morales, M. T.; Alonso, M. V. Relationship between volatile compounds and sensory attributes of olive oils by the sensory wheel. *J. Am. Oil Chem. Soc.* **1996**, *73*, 1253–1264.

(28) Morales, M. T.; Luna, G.; Aparicio, R. Sensory and chemical evaluation of winey-vinegary defect in virgin olive oils. *Eur. Food Res. Technol.* **2000**, *211*, 222–228.

(29) Linforth, S. T. Modelling flavour release. In *Food Flavour Technology*; Taylor, A. J., Linforth, S. T., Eds.; Wiley: Oxford, U.K., 2010; pp 207−228.

(30) Ryan, P. B.; Barr, L. B.; Todd, H. D. Simplex techniques for nonlinear optimization. *Anal. Chem.* **1980**, *52*, 1460–1467.

(31) Poellinger, A.; Thomas, R.; Lio, P.; Lee, A.; Makris, N.; Rosen, B. R.; Kwong, K. K. Activation and habituation in olfaction - An fMRI study. *NeuroImage* **2001**, *13*, 547–560.

(32) Van de Moortele, P. F.; Cerf, B.; Lobel, E.; Paradis, A. L.; Faurion, A.; Le Bihan, D. Latencies in fMRI time series: effect of slice acquisition order and perception. *NMR Biomed.* **1997**, *10*, 230–236.

(33) Grabenhorst, F.; Rolls, E. T.; Margot, C.; da Silva, M. A.; Velazco, M. I. How pleasant and unpleasant stimuli combine in different brain regions: Odor mixtures. *J. Neurosci.* **2007**, *27*, 13532–13540.

(34) García-Falgueras, A.; Junque, C.; Giménez, M.; Caldú, X.; Segovia, S.; Guillamon, A. Sex differences in the human olfactory system. *Brain Res.* **2006**, *1116*, 103–111.

(35) Koizuka, I.; Yano, H.; Nagahara, M.; Mochizuki, R.; Seo, R.; Shimada, K.; Kubo, T.; Nogawa, T. Functional imaging of the human olfactory cortex by magnetic resonance imaging. *ORL J. Otorhinolaryngol. Relat. Spec.* **1994**, *56*, 273–275.

(36) Cutting, L. E.; Clements, A. M.; Courtney, S.; Rimrodt, S. L.; Schafer, J. G. B.; Bisesi, J.; Pekar, J. J.; Pugh, K. R. Differential components of sentence comprehension: Beyond single word reading and memory. *NeuroImage* **2006**, *29*, 429–438.

(37) Savic, I.; Berglund, H. Passive perception of odors and semantic circuits. *Hum. Brain Mapp.* **2004**, *21*, 271–278.

(38) Uher, R.; Murphy, T.; Friederich, H. C.; Dalgleish, T.; Brammer, M. J.; Giampietro, V.; Phillips, M. L.; Andrew, C. M.; Ng, V. W.; Williams, S. C. R.; Campbell, I. C.; Treasure, J. Functional neuroanatomy of body shape perception in healthy and eating-disordered women. *Biol. Psychiatry* **2005**, *58*, 990–997.

(39) Eugène, F.; Lévesque, J.; Mensour, B.; Leroux, J. M.; Beaudoin, G.; Bourgouin, P.; Beauregard, M. The impact of individual differences on the neural circuitry underlying sadness. *NeuroImage* **2003**, *19*, 354–364.

(40) Fulbright, R. K.; Skudlarski, P.; Lacadie, C. M.; Warrenburg, S.; Bowers, A. A.; Gore, J. C.; Wexler, B. E. Functional MR imaging of regional brain responses to pleasant and unpleasant odors. *Am. J. Neuroradiol.* **1998**, *19*, 1721–1726.

(41) Miyanari, A.; Kaneoke, Y.; Noguchi, Y.; Honda, M.; Sadato, N.; Sagara, Y.; Kakigi, R. Human brain activation in response to olfactory stimulation by intravenous administration of odorants. *Neurosci. Lett.* **2007**, *423*, 6–11.